Zero-point entropy in 'spin ice'

A. P. Ramirez*, A. Hayashi†, R. J. Cava†, R. Siddharthan‡ & B. S. Shastry‡

* *Bell Laboratories, Lucent Technologies, 600 Mountain Avenue, Murray Hill, New Jersey 07974, USA*

† *Chemistry Department, Princeton University, Princeton, New Jersey 08540, USA*

‡ *Department of Physics, Indian Institute of Science, Bangalore 560012, India*

Common water ice (I_h) is an unusual solid—the oxygen atoms form a periodic structure but the hydrogen atoms are highly disordered due to there being two inequivalent O–H bond lengths[1]. Pauling showed that the presence of these two bond lengths leads to a macroscopic degeneracy of possible ground states[2,3], such that the system has finite entropy as the temperature tends towards zero. The dynamics associated with this degeneracy are experimentally inaccessible, however, as ice melts and the hydrogen dynamics cannot be studied independently of oxygen motion[4]. An analogous system[5] in which this degeneracy can be studied is a magnet with the pyrochlore structure—termed 'spin ice'—where spin orientation plays a similar role to that of the hydrogen position in ice I_h. Here we present specific-heat data for one such system, $Dy_2Ti_2O_7$, from which we infer a total spin entropy of $0.67R\ln 2$. This is similar to the value, $0.71R\ln 2$, determined for ice I_h, so confirming the validity of the correspondence. We also find, through application of a magnetic field, behaviour not accessible in water ice—restoration of much of the ground-state entropy and new transitions involving transverse spin degrees of freedom.

The problem of hydrogen-ordering in ice is perhaps the first example of geometrical frustration, by now a familiar concept in magnetism[6], where suppression of long-range magnetic order arises from the incompatibility of local and global symmetries. The simplest such case is realized for uniaxial spins interacting antiferromagnetically on a two-dimensional triangular lattice. This system does not order magnetically at any finite temperature and has, theoretically, a finite ground-state entropy[7]. In ice I_h, geometrical frustration arises from the incompatibility of the local bonding distances with long-range oxygen order. The oxygens form a periodic lattice isomorphic to the centre of the tetrahedra in the pyrochlore structure shown in Fig. 1. The O–O bond length is 2.75 Å, which is greater than twice the covalent O–H distance of 1.00 Å. In order to reconcile the crystal structure of ice I_h with the known bond lengths, Bernal and Fowler[1] formulated the so-called ice rules, which stipulate that two of the four hydrogen ions surrounding each oxygen ion sit closer to the oxygen ion than the other two. For every tetrahedron, there are six ways of achieving this lowest energy state and because the tetrahedra are corner-sharing, the associated degeneracy can not be lifted by long-range order. Pauling showed[2] that this leads to residual "macroscopic" ground-state entropy per H of $(1/2)R\ln(3/2) = 1.68\,\mathrm{J\,mol^{-1}\,K^{-1}}$. This idea resolved a discrepancy between the spectroscopically determined entropy at 298 K and that determined by direct calorimetric measurements[3]. Although the H-disorder can be represented as ground-state entropy, there is no clear violation of the third law of thermodynamics because the energetic barriers to establishing long-range order are of the order ~1 eV, which makes relaxation through tunnelling into a lower entropy state an extremely slow process below ice's freezing temperature.

The analogous magnetic situation is one where the two H-positions (close to, and far from, an O atom) are represented by the two states of spin-1/2 atomic moments, which reside on a lattice of corner-shared tetrahedra, as in the pyrochlore lattice (Fig. 1). Additional requirements for the analogy are that the spins lie along an axis (Ising-type) joining the tetrahedron vertex with its centre, and that they interact ferromagnetically. Harris *et al.*[5] showed that in this case, the lowest energy state for each tetrahedron is one where two spins point outwards and two point inwards, a state which has the same degeneracy as ice I_h. This situation is realized in the rare-earth (RE) titanate pyrochlores $RE_2Ti_2O_7$ where RE is Dy^{3+} or Ho^{3+}. (Dy^{3+} has effective spin $\tilde{S} = 1/2$ and an effective g-factor governing Zeeman splitting of the ground-state doublet $g_{\mathrm{eff}} \approx 9$ along the Ising axis. The next highest excited state is expected to be around 200 K.) The Ising nature of Dy and Ho is to be contrasted with the more common Heisenberg (or x–y) types of spin, where vector character is manifested in a continuous range of possible spin orientations and where, consequently, ice rules do not apply. Systems where such spins are situated in structures which are (like the pyrochlore lattice) both underconstrained in the Maxwellian sense[8] and triangle-based also have large ground-state degeneracy, and are said to be geometrically frustrated[6,9]. The analogy of the Ising-spin system with ice I_h has led Harris *et al.* to call this system "spin ice"[5]—its advantage over ice I_h is that the structure is stable at temperatures greater than the average interaction strength, allowing the study of the development of the degenerate ground state.

The $Dy_2Ti_2O_7$ sample used in the present measurements of heat capacity (C) as a function of temperature (T) was a ceramic powder prepared by standard solid-state synthesis techniques. The starting materials—Dy_2O_3 (99.99%) powder and TiO_2 (99.995%) powder—were mixed in stoichiometric proportions and heated in air at 1,200 °C for 4 days. For $C(T)$ measurements, the resulting powder was cold-sintered into a hard disk with Ag powder to facilitate thermal equilibration. The mass of $Dy_2Ti_2O_7$ in the disk was determined by measuring d.c.-susceptibility, χ_{dc}, above 2 K, and compared to a sample of precisely known mass. The Ag contribution to $C(T)$ was measured separately and subtracted from all data; at 1 K it represented only 0.4% of the total heat capacity. A standard semiadiabatic heat pulse technique was used with an equilibration time window of 15 s. Below 0.5 K in zero field and at lower T in finite fields, the internal relaxation time merged with the external relaxation time mostly as a result of a very small $C(T)$, and thus $C(T)$ was not well defined below $T \approx 0.2$ K.

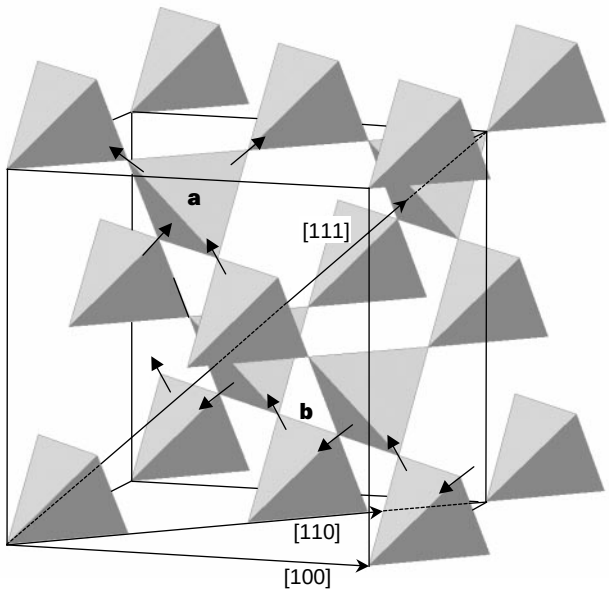

Figure 1 A section of the pyrochlore lattice, with the unit cell shown. Also shown are the principal crystal axes and two different spin configurations, discussed in the text, for Dy spins which lie on the vertices of the tetrahedra. Panel **a** shows the ground-state configuration of ferromagnetically interacting Ising spins on a tetrahedron. Panel **b** shows part of the subfamily of spins which do not couple to a field along (110).

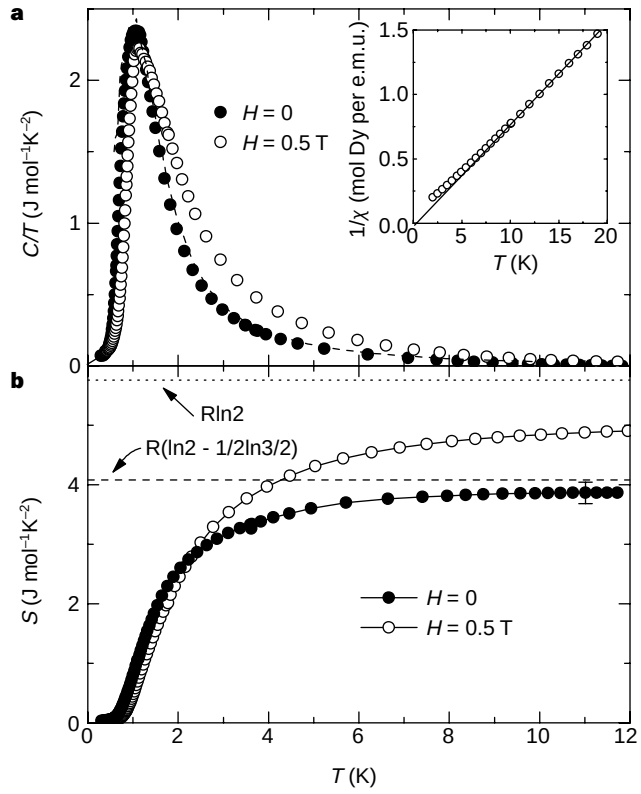

Figure 2 Specific heat and entropy of the spin-ice compound $Dy_2Ti_2O_7$ showing agreement with Pauling's prediction for the entropy of water ice I_h, $R(\ln 2 - (1/2)\ln(3/2))$. **a**, Specific heat divided by temperature of $Dy_2Ti_2O_7$ in $H = 0$ and 0.5 T. The dashed line is a Monte Carlo simulation of the zero-field $C(T)/T$, as discussed in the text. **b**, Entropy of $Dy_2Ti_2O_7$ found by integrating C/T from 0.2 to 14 K. The value of $R(\ln 2 - (1/2)\ln(3/2))$ is that found for ice I_h and $R\ln 2$ is the full spin entropy. Inset, susceptibility (M/H) of $Dy_2Ti_2O_7$ in a field of 0.02 T.

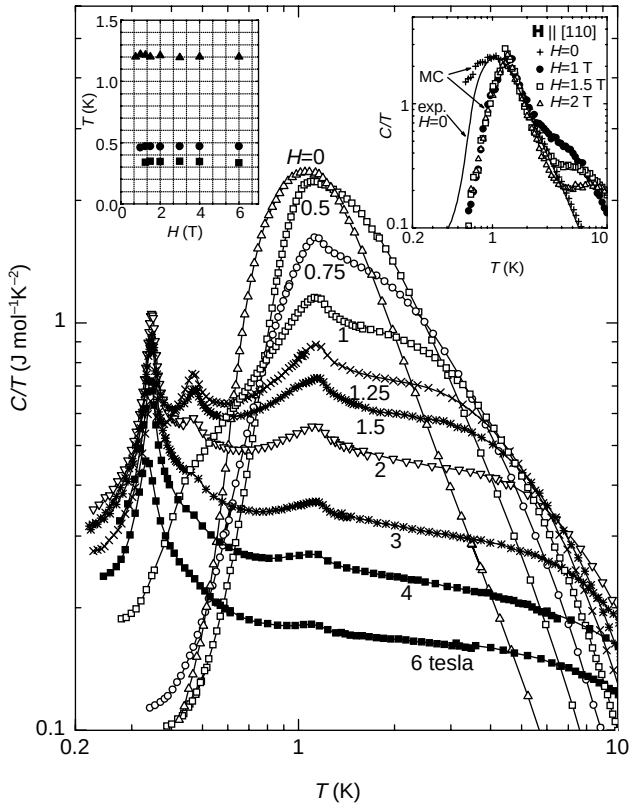

Figure 3 Specific heat versus temperature for various values of applied field. The broad $H = 0$ feature is suppressed on increasing H and replaced by three sharp features at 0.34, 0.47 and 1.12 K. The left inset shows the constancy of these transition temperatures with field; the right inset shows the results of finite-field Monte Carlo (MC) simulations of C/T.

In Fig. 2a inset we show $\chi_{dc}(T)$ from 2 to 20 K, illustrating the small ferromagnetic, FM, intercept, corresponding to a Weiss constant $\theta_w \approx 0.5$ K, where $1/\chi = \text{const.}/(T - \theta_w)$. The $C(T)/T$ data, which extend down to lower temperatures (Fig. 2a), show a much broader peak than usually seen for an antiferromagnetic, AF, transition. The lack of a clear ordering feature in $C(T)$ is consistent with a picture where the spins 'freeze' in a random configuration as a result of geometrical frustration. The absence of magnetic order in a system with no structural disorder is by itself unusual. The first reported example of such a system is another pyrochlore compound, $Y_2Mo_2O_7$, where despite the absence of any measured structural disorder, long-range magnetic order is not observed[10]—instead, spin glass freezing among Heisenberg-like Mo^{4+} ions sets in at $T \approx 0.3\theta_w \approx 15$ K. But existing susceptibility measurements[11] on $Dy_2Ti_2O_7$ do not show the sharp cusp expected for a spin glass, but rather a broad feature peaked at $T \approx 0.7$ K, indicating a different type of frozen spin state for this Ising-type spin system.

The most surprising aspect of our data, however, is found when integrating $C(T)/T$ from 0.2 to 12 K to obtain the total spin entropy (Fig. 2b). This temperature range incorporates all appreciable observed contributions to $C(T)/T$. We obtain $\Delta S(0.2, 12) = (0.67 \pm 0.04)R\ln 2$, that is, a shortfall of $\sim$1/3 of the total spin entropy. It has been previously noted, based on measurements of $C(T)$ only up to 1.5 K and a numerical extrapolation to higher temperatures, that the peak height is consistent with reduced entropy[11]: but it was suggested that the extrapolation was too simple, and that the missing entropy would be found for $T > 1.5$ K. We see no evidence for missing entropy for $T > 1.5$ K and, although it is possible that additional entropy is developed below 0.2 K, we think it unlikely for the following reasons. First, $C(T)/T$ drops by almost two orders of magnitude from 1 to 0.5 K indicating near-complete spin freezing, and second, there is no structural reason to assume a bimodal distribution of entropy-loss processes, for example, due to two different exchange interactions. In addition, our Monte Carlo simulation reproduces the observed $C(T)/T$ peak height and shape (Fig. 2a). (The Monte Carlo simulation was performed on a sample of size $8 \times 8 \times 8$ tetrahedra (2,048 spins) and $\sim 10^4$ Monte Carlo steps per spin. The spin–spin interaction was assumed to be purely dipole–dipole but with a g-factor reduced by 25% from the $J = 15/2$ Lande value. This is most likely the result of the compensating effect of a small admixture of superexchange interaction. Justification for this, and further details, will be given elsewhere (A.P.R. *et al.*, manuscript in preparation).

The comparison of the measured entropy with the prediction of Pauling for ice I_h, $R(\ln 2 - (1/2)\ln(3/2))$, is shown in Fig. 2b. To test the idea that there exists a contribution to ground-state entropy from a different energetically unfavoured state, we applied a small magnetic field, H, to reduce the energy barriers for spin reorientation. As shown in Fig 2a and b, an applied field of 0.5 T results not only in a shift of $C(T)/T$ to higher temperatures, but also in an increase of the integrated entropy, $\Delta S(0.2, 12)$, from $0.67R\ln 2$ to $0.85R\ln 2$. The increase of temperature where $C(T)/T$ is appreciable is expected, because Zeeman splitting increases with field. The increase of total ΔS, however, underscores the existence of additional entropy beyond that contained in the $H = 0$ peak. The

energetic barriers to spin reorientation, which are presumably due to geometrical frustration, are effectively lowered in finite field. The analogous experiment to recover missing entropy by application of pressure has not been performed in ice I_h, to our knowledge, although KOH-doping induces a transition which seems to restore nearly all of the missing entropy[12].

For applied fields larger than 1 T, additional features develop in $C(T)/T$ in the form of three sharp peaks at $T = 0.34$, 0.47 and 1.12 K (Fig. 3). These peaks are unusual in two respects. First, they represent only a few per cent of the total spin entropy—this is most likely to be due to the polycrystalline nature of the sample, as discussed below. Second, the peak positions do not depend on the magnitude of the applied field. This field-independence is shown in Fig. 3, left inset. We note that, independent of the details of possible spin-ordering models, these peaks can not be due to longitudinal spin fluctuations—they are still observable at $H = 6$ T where the Zeeman energy for longitudinal spins is ~55 K, that is, a Boltzmann factor $g\mu_B\tilde{S}H/k_BT$ of 157 for the lowest-temperature peak.

The occurrence of sharp peaks in thermodynamic quantities in finite field when there are none in zero field is rare, and to our knowledge has been seen previously only in the frustrated magnet $Gd_3Ga_5O_{12}$ (refs 13, 14) and low-dimensional spin systems[15]. In contrast to both of these examples, the peak temperatures in $Dy_2Ti_2O_7$ are field-insensitive. Harris *et al.* have recently reported[16] Monte Carlo simulations of $C(T)$ for the pyrochlore ferromagnet. These workers found, on application of a finite field $\mathbf{H}\|[100]$, a sharp spike in $C(T)$; the temperature corresponding to the peak of this spike also varied with applied field, indicating a different type of transition to that which we observe in $Dy_2Ti_2O_7$.

We propose that the $Dy_2Ti_2O_7$ peaks are due to correlated motion among spins which do not couple to the magnetic field, a situation realized for $\mathbf{H}\|[100]$ where half the spins have their Ising axis oriented perpendicular to $\mathbf{H}$. In this case, for $g\mu|\mathbf{H}| \gg k_B\theta_w$, the disorder of the ice state will be suppressed, leading to ordering on the sublattice of field-decoupled spins, which form chains as shown in Fig. 1. This model is supported by our own Monte Carlo calculations which show that for $\mathbf{H}\|[100]$, a sharp field-independent peak develops at a temperature corresponding to that of the upper peak in the $Dy_2Ti_2O_7$ data (Fig. 3, right inset). The observed lower-T transitions are possibly long-wavelength reordering processes which are not reproduced in Monte Carlo simulations owing to the small sample size in such simulations. Finally, we note that the peak heights in our orientationally averaged powder sample are significantly less than expected from ordering among half the spins. This suggests that there will need to be tight constraints on the sample orientation in future experiments on single crystals. □

Received 16 February; accepted 29 March 1999.

1. Bernal, J. D. & Fowler, R. H. A theory of water and ionic solution, with particular reference to hydrogen and hydroxyl ions. *J. Chem. Phys.* **1,** 515–548 (1933).
2. Pauling, L. *The Nature of the Chemical Bond* 301–304 (Cornell Univ. Press, Ithaca, New York, 1945).
3. Giauque, W. F. & Stout, J. W. The entropy of water and the third law of thermodynamics. The heat capacity of ice from 15 to 273K. *J. Am. Chem. Soc.* **58,** 1144–1150 (1936).
4. Hobbs, P. V. *Ice Physics* (Clarendon, Oxford, 1974).
5. Harris, M. J., Bramwell, S. T., McMorrow, D. F., Zeiske, T. & Godfrey, K. W. Geometrical frustration in the ferromagnetic pyrochlore $Ho_2Ti_2O_7$. *Phys. Rev. Lett.* **79,** 2554–2557 (1997).
6. Ramirez, A. P. Geometrical frustration in magnetism. *Annu. Rev. Mater. Sci.* **24,** 453–480 (1994).
7. Wannier, G. H. Antiferromagnetism. The triangular Ising net. *Phys. Rev.* **79,** 357–364 (1950).
8. Moessner, R. & Chalker, J. T. Low-temperature properties of classical geometrically frustrated antiferromagnets. *Phys. Rev. B* **58,** 12049–12062 (1998).
9. Schiffer, P. & Ramirez, A. P. Recent experimental progress in the study of geometrical magnetic frustration. *Comments Cond. Mat. Phys.* **18,** 21–50 (1996).
10. Greedan, J. E., Sato, M., Yan, X. & Razavi, F. S. Spin-glass-like behavior in $Y_2Mo_2O_7$, a concentrated, crystalline, system with negligible apparent disorder. *Solid State Commun.* **59,** 895–897 (1986).
11. Blöte, H. W. J., Wielinga, R. F. & Huiskamp, W. J. Heat-capacity measurements on rare-earth double oxides $R_2M_2O_7$. *Physica* **43,** 549–568 (1969).
12. Tajima, Y., Matsuo, T. & Suga, H. Phase transition in KOH-doped hexagonal ice. *Nature* **299,** 810–812 (1982).
13. Schiffer, P., Ramirez, A. P., Huse, D. A. & Valentino, A. J. Investigation of the field induced antiferromagnetic phase transition in the frustrated magnet: gadolinium gallium garnet. *Phys. Rev. Lett.* **73,** 2500–2503 (1994).
14. Hov, S., Bratsberg, H. & Skjeltorp, A. T. Magnetic phase diagram of gadolinium gallium garnet. *J. Magn. Magn. Mater.* **15–18,** 455–456 (1980).
15. Manaka, H., Yamada, I., Honda, Z., Katori, H. A. & Katsumata, K. Field-induced magnetic long-range order in the ferromagnetic-antiferromagnetic alternating heisenberg chain system $(CH_3)_2CHNH_3CuCl_3$ observed by specific heat measurements. *J. Phys. Soc. Jpn* **67,** 3913–3917 (1998).
16. Harris, M. J., Bramwell, S. T., Holdsworth, P. C. W. & Champion, J. D. M. Liquid-gas critical behavior in a frustrated pyrochlore ferromagnet. *Phys. Rev. Lett.* **81,** 4496–4499 (1998).

Acknowledgements. We thank C. Ulrich for assistance, and C. Broholm, P. Chandra, A. P. Mills, R. Moessner, J. A. Mydosh, C. M. Varma and W. P. Wolf for discussions.

Correspondence and requests for materials should be addressed to A.P.R. (e-mail: apr@bell-labs.com).

A thermoacoustic Stirling heat engine

S. Backhaus & G. W. Swift

Condensed Matter and Thermal Physics Group, Los Alamos National Laboratory, Los Alamos, New Mexico 87545, USA

Electrical and mechanical power, together with other forms of useful work, are generated worldwide at a rate of about 10^{12} watts, mostly using heat engines. The efficiency of such engines is limited by the laws of thermodynamics and by practical considerations such as the cost of building and operating them. Engines with high efficiency help to conserve fossil fuels and other natural resources, reducing global-warming emissions and pollutants. In practice, the highest efficiencies are obtained only in the most expensive, sophisticated engines, such as the turbines in central utility electrical plants. Here we demonstrate an inexpensive thermoacoustic engine that employs the inherently efficient Stirling cycle[1]. The design is based on a simple acoustic apparatus with no moving parts. Our first small laboratory prototype, constructed using inexpensive hardware (steel pipes), achieves an efficiency of 0.30, which exceeds the values of 0.10–0.25 attained in other heat engines[5,6] with no moving parts. Moreover, the efficiency of our prototype is comparable to that of the common internal combustion engine[2] (0.25–0.40) and piston-driven Stirling engines[3,4] (0.20–0.38).

We plan to acoustically couple our thermoacoustic Stirling engines to pulse tube refrigerators[7], to provide efficient and maintenance-free combustion-powered cryogenic refrigeration having no moving parts, in order to liquefy natural gas[8]. This would enable economic recovery of 'associated gas', a by-product of oil production, which is currently burned ('flared') in vast quantities at remote oil fields worldwide, wasting fossil fuel and contributing to global warming. We expect our engine to find many additional uses throughout the global power-production environment, ranging from the separation of air into nitrogen and oxygen to the generation of electricity.

Ceperley[9,10] made the initial step towards this new engine, when he realized that gas in an acoustic travelling wave propagating through a regenerative heat exchanger (regenerator) undergoes a thermodynamic cycle similar to the ideal Stirling cycle; this is because the oscillations of pressure (p_1) and volumetric velocity (U_1) are temporally in phase in a travelling wave. We use the conventional anticlockwise phasor notation[11], so that time-dependent variables are expressed as

$$\xi(t) = \xi_m + \mathrm{Re}[\xi_1 e^{i\omega t}] \quad (1)$$

with the mean value ξ_m real, and with ξ_1 complex, to account for both the magnitude and phase of the oscillation at angular frequency ω. The net work performed in the cycle manifests itself as an increase in the time-averaged acoustic power $\dot{W} = \mathrm{Re}[p_1\tilde{U}_1]/2$ of the wave as it passes through the regenerator. (The tilde denotes complex conjugate.) Although Ceperley's experiments never achieved power gain, he provided a key insight[12] for constructing a useful thermoacoustic Stirling engine. If a pure travelling wave were used, the ratio of acoustic pressure to volume velocity would be